

Organic-Inorganic Hybrid Electrolytes for High Temperature PEFCs

Jedeok Kim^{1*}, Toshiyuki Mori¹, and Itaru Honma²

¹Fuel Cell Materials Center, National Institute for Materials Science (NIMS), 1-1 Namiki Tsukuba-shi, Ibaraki 305-0044, Japan

Fax: 81-29-860-4667, e-mail: Kim.Jedeok@nims.go.jp

²Energy Technology Research Institute, National Institute of Advanced Industrial Science and Technology (AIST), 1-1-1 Umezono, Tsukuba-shi, Ibaraki 305-8568, Japan

Organic-inorganic proton electrolytes were investigated by the cross-linking of various organic monomers (PDMS, PTMO) and metal (Zr, Ti) alkoxides. Proton conductors of 12-phosphotungstic (PWA) and phosphoric acids interacted with inorganic phase of organic-inorganic hybrids. Some hybrids showed high mechanical and thermal stability up to 300 °C. Moreover, high proton conducting hybrids were investigated a cell performance using single MEA cell. The organic-inorganic conducting hybrids, which have high proton conductivity and thermal stability, can be expected for applications in intermediate temperature PEFCs.

Key words: Organic-inorganic, hybrid membrane, proton electrolytes, thermal stability, intermediate temperature PEFCs.

1. Introduction

Polymer electrolyte membrane fuel cells (PEMFCs) have been investigated extensively as a future energy source to solve a global energy and environmental problem due to their high energy conversion efficiency. PEMFCs at low temperatures (below 80 °C) using hydrated perfluorosulfonic polymers such as Nafion have been developed in the past years for mobile, satellite or stationary applications. Currently, it is expected that energy conversion devices in the future that have higher energy efficiency than membrane fuel cells will become a leading alternative to internal combustion and diesel engines. However, the high materials cost and complicated water management are major obstacles for practical applications of PEMFCs. Moreover, carbon monoxide, which is contained in the hydrogen gas reformed by hydrocarbons such as natural gas, gasoline, or alcohol at the ppm level, can severely poison the anode catalyst of membrane electrolyte assembly (MEA) and can cause significant loss in energy efficiency. On the

other hand, the operation of PEMFCs at intermediate temperatures (100 - 200 °C) has been considered to provide many advantages such as improved CO tolerance of the Pt electrode [1-4], reduction of the amount of Pt electrode materials [5], higher energy efficiency, better heat management, co-generation, and suppression of flooding in MEA. Many temperature tolerant polymer materials have been synthesized, and protonic conductivity and cell performance at elevated temperature ranges have been investigated intensively [6-41].

On the other hand, the sol-gel process has been used for the preparation of crystalline and non-crystalline ceramic oxides and glasses. The materials possess remarkable isotropic, flexibility and functional properties originating from organic and inorganic moieties. Additionally, they can be synthesized through an easy processing route with low cost and reduced environmental impacts [42-48]. On the other hand, organic-inorganic hybrid materials can become proton and/or lithium ion conductors by

controlling the molecular structure of the hybrids, and the hybrids incorporated with proton conductors can be applied to fuel cells and battery electrolytes [6-8,10-16,18-20,26-29,34-37,41,48-54]. The organic structure as well as a novel synthetic route have been investigated to enable fast ionic conduction through molecular modification of organic ligand to inorganic structures [6-18,22-41,48-57].

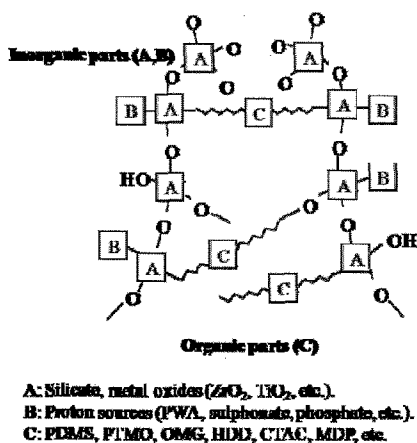


Fig. 1 Schematic diagram for the design of an organic-inorganic proton conductor.

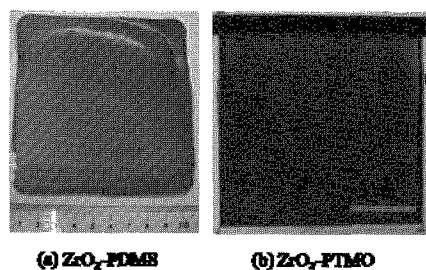


Fig. 2 Photographs of organic-inorganic hybrid membranes.

Fig. 1 shows a schematic diagram for a design of organic-inorganic proton conductor. The organic-inorganic interfaces can be formed by sol-gel processing of end groups (OH) of organic parts with reactive inorganic parts to afford hybrids at molecular scale. Moreover, the hybrid material becomes proton electrolytes by incorporation of proton sources such as phosphotungstic (PWA) or phosphate acids. Polyanion

PWA clusters have been incorporated with inorganic silica framework and they never dissociate from the hybrid matrix. Effects of PWA doping concentration on the thermal stability and protonic conductivity are discussed in other papers [6,48].

Here we reported the synthesis, thermal and chemical stabilities, conducting property and cell performance of organic-inorganic proton hybrids using organic monomers (PDMS, PTMO), metal (Zr, Ti) alkoxides, and PWA and phosphoric acids.

2. Experimental

PDMS (liquid Mw = 4500, GE Toshiba Silicon Co. Ltd. and Mw = 600, Gelest Inc.) and PTMO (liquid Mw = 650, Wako Chemical Co. Ltd.) were used as organic monomers. $[Zr(OCH(CH_3)_2)_4 \cdot (CH_3)_2CHOH]$ (Alfa Co. Ltd), $Ti(OC_2H_5)_4$, PWA (Wako Chemical Co. Ltd.) and H_3PO_4 were used as inorganic and proton materials. An ethyl acetoacetate (eacac) solution was added to the zirconium isopropoxide to stabilize the sol and to prevent a rapid hydrolysis. The metal alkoxide and eacac were mixed in ethanol or isopropanol solution and stirred for 30 min, then, organic monomers were added with vigorous stirring. In the case of PWA, PWA in the ethanol solution was added to the above sol and stirred another 30 min. The sol was cast onto a Petri dish and subjected to aging at 100 °C for 2 – 5 days to yield a hybrid gel. The gel was further annealed at 180 °C for 1 – 3 days to form organic-inorganic hybrid membrane. The heat-treated hybrid membranes were soaked at H_3PO_4 solution. The thickness of membrane was depended on the sol volume. Fig. 2 showed transparent and flexible organic-inorganic hybrid membranes.

The chemical bonding of the hybrids was measured by FTIR (FT/IR-6200 with ATR Pro 410-S, JASCO). Thermogravimetry-differential thermal analyses (TG-DTA) of the samples were conducted to characterize

the thermal stability of hybrid samples at a heating rate of 20 °C/min under air or N₂ atmosphere. Dynamic elastic modulus and dissipation ($\tan\delta$) of the hybrid membranes were measured by EXSTAR6000 dynamic viscoelastometer (Seiko Instruments, Inc.) at 10 Hz in the temperature range from 25 to 250 °C at a heating rate of 3 °C/min. ³¹P-MASNMR has been employed for characterization of the phosphorous microenvironment of zirconia phosphate or titania-PWA in organic-inorganic proton conductor structures. The ³¹P-MASNMR spectra were obtained at 121.532 MHz on a Fourier Transform pulsed NMR spectrometer (Chemagnetics CMX-300). The conditions of pulse width, pulse delay and spinning speeds were 1.5 μsec, 60 sec and 10 kHz, respectively. The proton conductivity was measured by two-terminal impedance spectroscopy (S1620 Impedance Analyzer, Solatron). The samples were placed between two ring-type gold plate blocking electrodes. A frequency range of 1 Hz to 1 MHz and a peak-to-peak voltage of 10 mV were used for the impedance measurements. When the conductivity of the membrane was measured at higher temperatures, the apparatus cell was pressurized to maximum 0.5 MPa (150 °C) in order to keep saturated humidity. To get cell performance, ZrO₂/PTMO/H₃PO₄ hybrid membranes were prepared by impregnating over 7 days with 1M H₃PO₄. The thickness of the membranes depended on the condition of sol-gel processing. On the other hand, TiO₂/PTMO/PWA hybrid was mixed with Nafion solution after grinding to get good membrane property, and TiO₂/PTMO/PWA-Nafion membrane was prepared by a mixing of TiO₂/PTMO/PWA hybrid with 5 wt% Nafion solution (Electrochem.). Commercially available gas-diffusion electrodes (20% Pt-on-carbon, 1mg Pt/cm², from Electrochem.) were impregnated with 5 wt% Nafion solution and then dried at 70 °C for 1h. The active area for the anode and cathode was 2.5 cm². A membrane was sandwiched between two electrodes, and

the resulting membrane electrode assembly (MEA) was then pressed at 4 MPa for 4 min at 130 °C. The MEA was coupled with gas-sealing gaskets and placed in a single cell test fixture. H₂ and O₂ (high purity gases) were fed to the single cell at controlled flow rate, humidity, temperature and pressure using a Fuel-Cell test station. In order to humidify the gases prior to entry to the fuel cell, H₂ and O₂ were bubbled through water in stainless steel bottles, the temperatures of which were individually controlled. The MEA was tested at various temperature with H₂ (0.1 l/min)/O₂ (0.1 l/min) under saturated humidity conditions. Performance evaluation curves were obtained with a computer-controlled SI1287 Electrochemical Interface (Solatron).

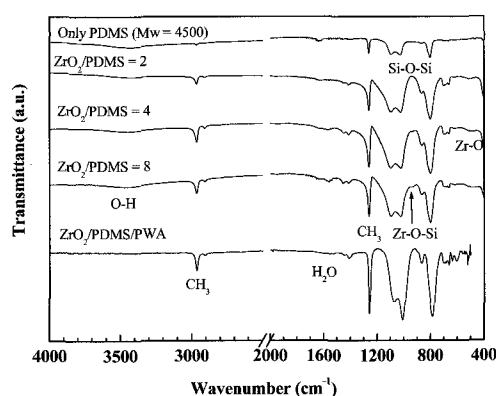


Fig. 3 FTIR spectra of ZrO₂/PDMS and ZrO₂/PDMS/PWA hybrids.

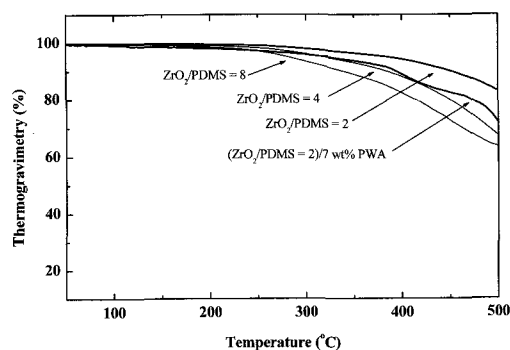


Fig. 4 TG results of ZrO₂/PDMS and ZrO₂/PDMS/PWA hybrids.

3. Results and Discussion

3.1 ZrO₂ (TiO₂)/PDMS/acid hybrid membranes

The molar ratio of ZrO₂ (TiO₂) to PDMS (Mw = 4500 and 600) was changed from 2 to 8, while the hybrid membranes were flexible, homogeneous, and transparent at those ratios. However, at higher metal oxide concentration, the membrane became brittle. On the other hand, the hybrid membranes synthesized with PWA was heterogeneous.

Fig. 3 showed FTIR spectra of the ZrO₂/PDMS and ZrO₂/PDMS/PWA hybrids. The peaks at 800 – 1100 cm⁻¹ can be attributed to the vibration of Si-O-Si bonds. The absorption peaks around 1600 and 3500 cm⁻¹ can be attributed to the deformation vibration of water H₂O and the stretching of hydroxyl groups O-H, respectively. On the other hand, an absorption peak corresponding to the Zr-O-Si bond was observed at 934 cm⁻¹. Also, Zr-O vibration appeared at 500 cm⁻¹. Therefore, the ZrO₂ was chemically bound to PDMS end groups via Zr-O-Si and Zr-O-Zr bonds. The membranes were recognized as macromolecules with interconnected phase of organic PDMS and inorganic zirconium oxide at nano-scale, resulting in a polymeric hybrid material. In the case of ZrO₂/PDMS/PWA hybrid, the fundamental vibration modes (P-O, W-O, W-O-W) of PWA keggin cluster structure have been seen in the wavenumbers of 1080, 976, and 900 cm⁻¹, respectively. However, the spectra can not easy to find due to the Si-O-Si spectra. However, it is speculated that the heteropoly acid has been successfully incorporated in the hybrid matrix due to the chemical shift of Si-O-Si spectra.

Fig. 4 showed TG of ZrO₂/PDMS (Mw = 4500) and ZrO₂/PDMS (Mw = 4500)/PWA hybrid membranes. The ZrO₂/PDMS/7 wt% PWA hybrid membrane showed homogeneous appearance. The thermal stability of ZrO₂/PDMS = 2 was better than that of other hybrids. The ZrO₂/PDMS/PWA hybrid was stable up to 300 °C.

The mechanical properties of the hybrid membranes were evaluated by dynamic elastic modulus measurement as shown in fig. 5. The hybrids had stable dynamic elastic modulus and tan δ with small change from 50 to 200 °C. However, the ZrO₂/PDMS/7 wt% PWA hybrid showed large tan δ due to the added PWA. The modulus of ZrO₂/PDMS = 2 and ZrO₂/PDMS/7 wt% PWA hybrids was lower than that of ZrO₂/PDMS = 4. The increase of inorganic phase in the hybrid might restrict the segmental motion of organic species and induce the strengthening of the network and as a result, the modulus of ZrO₂/PDMS = 4 was higher than that of ZrO₂/PDMS = 2.

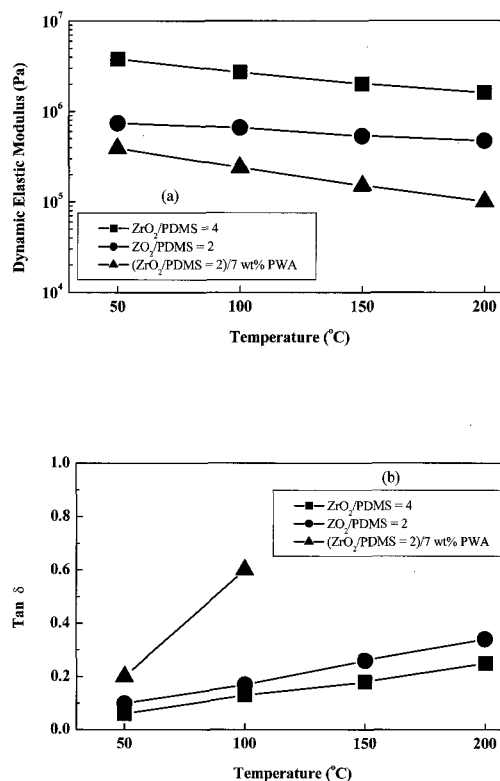


Fig. 5 Mechanical properties of ZrO₂/PDMS and ZrO₂/PDMS/PWA hybrids.

Fig. 6 showed temperature dependence for the conductivity of various ZrO₂ (TiO₂)/PDMS/PWA hybrids under the saturated humidity at each temperature. The ZrO₂ (TiO₂)/PDMS hybrid membrane showed small

proton conductivity in the order of 10^{-6} S/cm due to the Zr (Ti)-OH moiety. The conductivity of the hybrids increased due to the incorporated PWA. PWA exhibits preferential transport for positively charged ions, and does not transport also anions, if it is used to separate two electrolyte solutions (e.g. aqueous HCl) instead of being just put in a controlled humidity chamber. It is in fact highly probable that the described conductor is proton conducting only because protons are the only mobile species present in their experimental set-up. The conductivity of the hybrids was increased with increasing temperature and added PWA concentration. The proton conductivity of ZrO_2/PDMS ($M_w = 4500$)/PWA hybrids showed large temperature dependence. On the other hand, the conductivities of ZrO_2/PDMS ($M_w = 600$)/PWA and TiO_2/PDMS ($M_w = 600$)/PWA hybrids showed small temperature dependence due to the very small activation energy. On the other hand, the conductivity of TiO_2/PDMS ($M_w = 600$)/10 wt% PWA hybrid was higher than that of other hybrids. According to the previous results [48], it can be due to the formation of ion-conductive channels in the organic-inorganic hybrid macromolecules. Not only carrier density (proton) but also the mobility of ions predominantly affects the conductivity where the conductive pathways are greatly influenced by the dispersion state of PWA either a homogeneous mixture or bicontinuous network. Based on the evidence, although PWA contents were low, the conductivity of TiO_2/PDMS /10 wt% PWA hybrid could have higher than that of ZrO_2/PDMS /35 wt% PWA. The former might possess conductive bicontinuous pathways for protons through assembling PWA clusters at hydrophilic/hydrophobic interfaces. On the other hand, the ZrO_2/PDMS ($M_w=4500$)/21 wt% PWA hybrid showed extremely high proton conductivity with increasing temperature up to 150 °C, while the membrane slowly changed from solid to gel state. The membrane can be

provided continuous proton conducting channels under high humidity and pressure condition, resulting in an enhanced mobility of the protonic carriers such as H_3O^+ or H_5O_2^+ . We supposed that the gelation of ZrO_2 (TiO_2)/PDMS/PWA hybrids could be induced by the increased amount of PWA and relevant water content under high temperature and pressure condition, and provided the enhanced proton conductivity of the organic-inorganic hybrid materials.

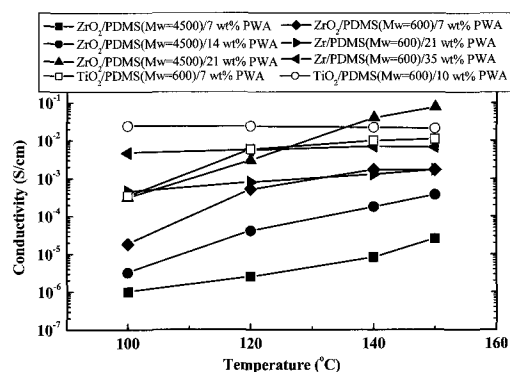


Fig. 6 Temperature dependence for the conductivity of ZrO_2 (TiO_2)/PDMS/PWA hybrids.

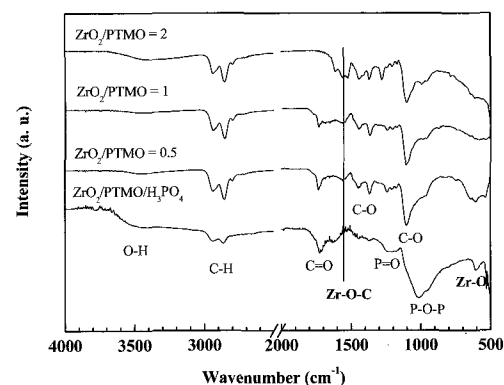


Fig. 7 FTIR spectra of ZrO_2/PTMO and $\text{ZrO}_2/\text{PTMO}/\text{H}_3\text{PO}_4$ hybrids.

3.2 ZrO_2 (TiO_2)/PTMO/acid hybrid membranes

The molar ratio of ZrO_2 (TiO_2) to PTMO ($M_w = 650$) was changed from 0.5 to 2. The hybrid membranes of ZrO_2/PTMO were flexible, homogeneous, and

transparent.

Fig. 7 showed IR spectra of $ZrO_2/PTMO$ and $ZrO_2/PTMO/H_3PO_4$ hybrid membranes. The absorption peak of covalently bonding of Zr-O-C and Zr-O was observed at 1560 and 530–600 cm^{-1} , respectively. In the case of $ZrO_2/PTMO/H_3PO_4$ hybrid, new bonding spectra due to the incorporated phosphoric acid appeared at the wavenumbers of 1620, 1245, 1031, and 950 cm^{-1} . The peaks could be assigned the vibration of bounded water, P=O, P-O, and P-O-P, respectively. From these results, it was speculated that $ZrO_2/PTMO$ hybrids became macromolecule structure, and phosphoric acid was successfully incorporated into the inorganic phase of $ZrO_2/PTMO$ hybrid.

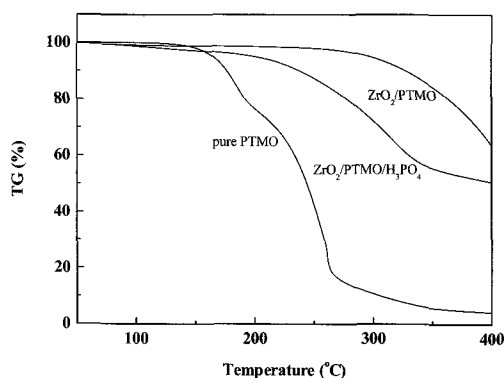


Fig. 8 TG results of $ZrO_2/PTMO$ and $ZrO_2/PTMO/H_3PO_4$ hybrids.

Fig. 8 showed thermal analysis (TG) of pure PTMO, $ZrO_2/PTMO$, and $ZrO_2/PTMO/H_3PO_4$ hybrid membranes, respectively. Thermal stability of $ZrO_2/PTMO$ hybrid was increased from 150 °C of pure organic PTMO to 250 °C due to the cross-linked matrix of organic PTMO and inorganic ZrO_2 phase at nano-scale. On the other hand, it of the $ZrO_2/PTMO/H_3PO_4$ hybrid was lower than that of $ZrO_2/PTMO$ hybrid. It could be due to the melting of an unreacted PTMO or chelated zirconium alkoxide/eacac into the H_3PO_4 solution. The initial weight loss (5%) of the sample could be attributed to desorption of surface

water and binded water from the membrane. From the results, the hybrid membranes had high thermal stability over 200 °C.

The mechanical properties of hybrid membranes were evaluated by dynamic elastic modulus measurements as shown in fig. 9. The storage modulus and $\tan \delta$ of the ZrO_2 (TiO_2)/PTMO and ZrO_2 (TiO_2)/PTMO/ H_3PO_4 hybrid membranes were shown in figs. 9(a) and 9(b), respectively. The storage modulus of $TiO_2/PTMO$ hybrid was higher than that of $ZrO_2/PTMO$. The moduli of ZrO_2 (TiO_2)/PTMO/ H_3PO_4 hybrids were higher than those of ZrO_2 (TiO_2)/PTMO due to the bonding of phosphoric acid in the inorganic phase.

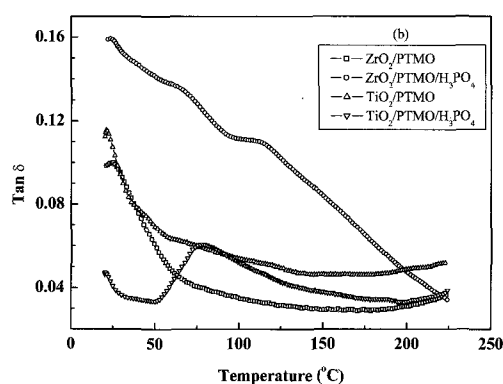
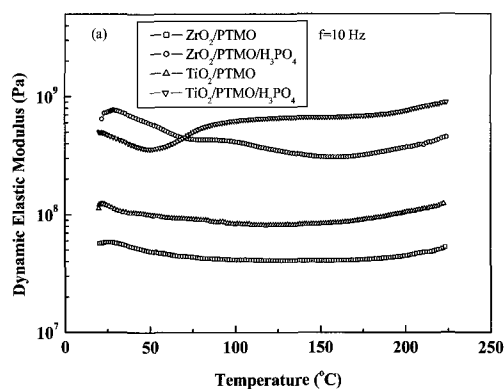


Fig. 9 Mechanical properties of $ZrO_2(TiO_2)/PTMO$ and $ZrO_2(TiO_2)/PTMO$ hybrids.

They showed a storage modulus of $10^8 - 10^9$ Pa. The ZrO_2 (TiO_2)/PTMO hybrids had a glass transition under

50 °C, and ZrO_2 (TiO_2)/PTMO/ H_3PO_4 hybrids showed more complex transition properties as shown in $\tan \delta$. The $\tan \delta$ of ZrO_2 /PTMO/ H_3PO_4 hybrid showed large temperature dependence. It can be due to the large swelling of phosphoric acid.

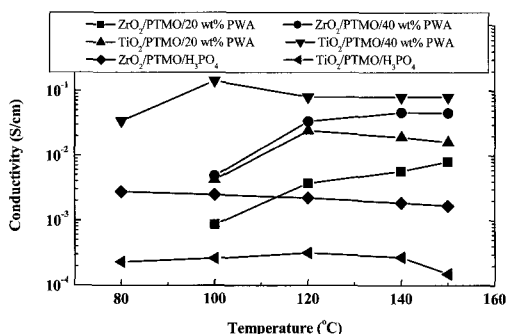


Fig. 10 Temperature dependence for the conductivity of ZrO_2 (TiO_2)/PTMO/PWA (H_3PO_4) hybrids.

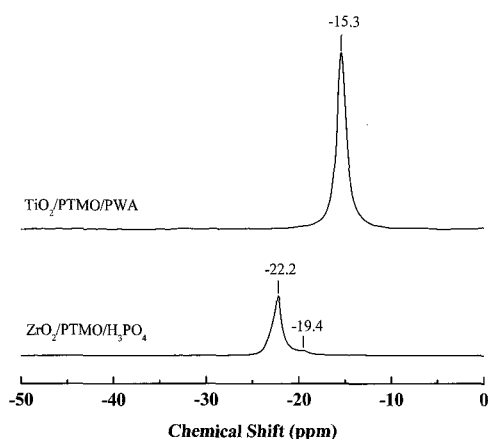


Fig. 11 ^{31}P MAS NMR spectra of TiO_2 /PTMO/PWA and ZrO_2 /PTMO/ H_3PO_4 hybrids.

Fig. 10 showed proton conductivities of ZrO_2 (TiO_2)/PTMO/PWA and ZrO_2 (TiO_2)/PTMO/ H_3PO_4 hybrid samples under the saturated humidity at each temperature. The conductivity of ZrO_2 /PTMO hybrid was very low (2×10^{-6} S/cm). The membrane became proton conductor when incorporated with PWA or H_3PO_4 . The conductivity of ZrO_2 (TiO_2)/PTMO/PWA hybrids was higher than that of ZrO_2 (TiO_2)/PTMO/ H_3PO_4 hybrids.

Moreover, temperature dependence of the ZrO_2 (TiO_2)/PTMO/PWA was larger than that of ZrO_2 (TiO_2)/PTMO/ H_3PO_4 hybrid. As the increasing of the temperature, the conductivity of TiO_2 /PTMO/40 wt% PWA hybrid was increased from 3×10^{-2} S/cm at 80 °C to 0.1 S/cm at 150 °C. The high conductivity of ZrO_2 (TiO_2)/PTMO/PWA hybrids at the high temperature is close to that of highly conductive ion-exchange membrane. It is speculated that the membrane was subjected to a structural change from solid to gel state under the saturated humidity and high temperature, and the high proton conductivity could be provided by the mobility of protonic carriers (H_3O^+ or $H_5O_2^+$) in the gel. On the other hand, the maximum proton conductivity of the ZrO_2 /PTMO/ H_3PO_4 hybrid was 3×10^{-3} S/cm. This value is two times lower than that of Nafion. Therefore, it is required higher proton conductivity.

To understand the local interaction and structure of proton conductor in organic/inorganic/acid hybrids, solid-state NMR spectroscopy analysis was investigated. Fig. 11 showed ^{31}P MAS NMR spectra of ZrO_2 /PTMO/ H_3PO_4 and TiO_2 /PTMO/PWA hybrid samples. The ^{31}P MAS NMR spectra of the ZrO_2 /PTMO/ H_3PO_4 hybrid showed a main chemical shift at -22.2 and -19.4 ppm. It is reported that the chemical shifts of $\epsilon-Zr(HPO_4)_2 \cdot H_2O$ and $Zr(HPO_4)_2 \cdot nH_2O$ -gel are at -19 ~ -21 ppm, and those of phosphoric acids and/or pyro-zirconium phosphates show at 0 ~ 5 and 50 ~ 60 ppm, respectively [58]. Therefore, it was speculated that ZrO_2 phase was mainly chemically bound to phosphoric acid through P-O-Zr bonding, resulting in immobilizing zirconium phosphate groups in the hybrid matrix. The NMR results indicated the phosphate moieties were strongly binding to inorganic phase. On the other hand, the solid state NMR of TiO_2 /PTMO/PWA hybrid also showed a strong interaction between heteropoly anion and inorganic TiO_2 phase. It was

reported that hexahydrated ($\text{H}_3\text{PW}_{12}\text{O}_{40}\cdot 6\text{H}_2\text{O}$) and anhydrous ($\text{H}_3\text{PW}_{12}\text{O}_{40}\cdot \text{H}_2\text{O}$) heteropoly acid forms gave a narrow peak at -15.6 and -11.0 ppm, respectively. The polyanions $[(\text{PW}_{12}\text{O}_{40})^{3-}]$ in the hexahydrate are packed in a cubic structure and all acidic protons are present in the form of H_3O_2^+ cations. [59] The $\text{TiO}_2/\text{PTMO}/\text{PWA}$ hybrid showed a peak at -15.3 ppm. The single peak indicated that polyanions were distributed homogeneously into TiO_2/PTMO hybrid. The chemical shift of the hybrid was to be between $\text{H}_3\text{PW}_{12}\text{O}_{40}\cdot 6\text{H}_2\text{O}$ and $\text{H}_3\text{PW}_{12}\text{O}_{40}\cdot 0\text{H}_2\text{O}$ due to a partial dehydration of heteropoly acid. Heteropoly acid crystallites should lose some of water molecules due to interactions and immobilization of heteropoly acid in the TiO_2/PTMO macromolecular structure. Some acidic protons of heteropoly acid should react with TiO_2 phase. It suggests that the interface of the hybrid have a $[\text{TiO}_x(\text{OH})_y][\text{H}_3\text{PW}_{12}\text{O}_{40}]$ structure, and the interaction could stabilize the heteropoly acid in TiO_2/PTMO hybrid matrix.

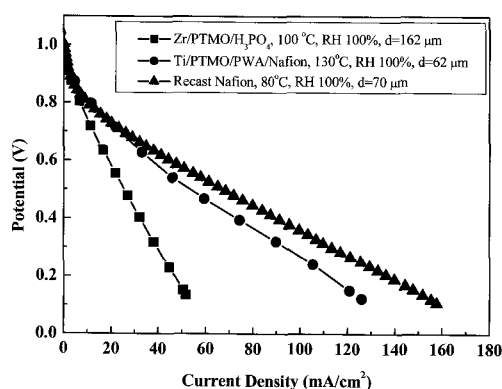


Fig. 12 Cell performance of hybrid membranes and recast Nafion.

Cell performance of $\text{ZrO}_2/\text{PTMO}/\text{H}_3\text{PO}_4$, $\text{TiO}_2/\text{PTMO}/\text{PWA}$ hybrid samples, and recast Nafion for some comparison was investigated by single MEA cell using PEFC system (Fig. 12). The $\text{TiO}_2/\text{PTMO}/40$ wt%

PWA hybrid showed the maximum conductivity of 8×10^{-2} S/cm between 120 and 150 °C under the saturated humidity condition. However, the hybrids could not get adequate size for MEA due to the brittleness. Therefore, Nafion gave support to the hybrid. The composite membrane of Nafion-hybrid was made by a mixing in the weight ratio of Nafion:hybrid=5:3. I - V performance of $\text{ZrO}_2/\text{PTMO}/\text{H}_3\text{PO}_4$, $\text{TiO}_2/\text{PTMO}/\text{PWA}/\text{Nafion}$, and recast Nafion was investigated at the temperature of 100 , 130 , and 80 °C under saturated humidity condition, respectively. The OCP of the samples was over 1.0 V. This means that the membranes did not have a porous or crack in the structure. The current density of recast Nafion was higher than that of the cell using $\text{ZrO}_2/\text{PTMO}/\text{H}_3\text{PO}_4$ and $\text{TiO}_2/\text{PTMO}/\text{PWA}/\text{Nafion}$ hybrid membranes. This is due to the difference of the membrane resistance. The $\text{ZrO}_2/\text{PTMO}/\text{H}_3\text{PO}_4$ and $\text{TiO}_2/\text{PTMO}/\text{PWA}/\text{Nafion}$ hybrids had maximum power density of 13 (at 100 °C) and 30 (at 130 °C) mW/cm^2 , respectively.

4. Conclusions

Organic-inorganic proton hybrid electrolytes have been synthesized by bridged macromolecules between metal alkoxides and organic monomers. The hybrid membranes showed superior thermal and mechanical properties because of the temperature tolerant organic-inorganic moieties and the nanostructure of the hybrid matrix. PWA and phosphoric acids were successfully incorporated in the inorganic interface as a proton source. ^{31}P MAS NMR displayed that the proton conductors such as PWA or phosphate were bonded with hydrophilic metal phases. The maximum proton conductivities for $\text{ZrO}_2/\text{PDMS}/\text{PWA}$, $\text{TiO}_2/\text{PTMO}/\text{PWA}$, and $\text{ZrO}_2/\text{PTMO}/\text{H}_3\text{PO}_4$ hybrids were 0.1 , and 1×10^{-3} S/cm under saturated humidity condition up to 150 °C, respectively. Moreover, it was obtained a power density

of 30 mW/cm² at the cell temperature of 130 °C. The organic-inorganic proton hybrid electrolytes could be expected to provide new technological applications in the electrochemical devices such as high temperature operation of polymer electrolyte fuel cell.

References

- [1] Q. Li, R. He, J.A. Gao, J.O. Jensen, and N.J. Bjerrum, *J. Electrochem. Soc.*, 150, 1599 (2003).
- [2] B.N. Grgur, N.M. Markovic, and P.N. Ross, *Electrochim. Acta*, 43, 3631 (1998).
- [3] S.J. Lee, S. Mukerjee, E.A. Ticianelli, and J. McBreen, *Electrochim. Acta*, 44, 3283 (1999).
- [4] Y. Si, R. Jiang, J.C. Lin, H.R. Kunz, and J.M. Fenton, *J. Electrochem. Soc.*, 151, 1820 (2004).
- [5] M.S. Wilson, J.A. Valerio and S. Gottesfeld, *Electrochim. Acta*, 40, 355 (1995).
- [6] I. Honma, H. Nakajima, and S. Nomura, *Solid State Ionics*, 154/155, 707 (2002).
- [7] P. Costamagna, C. Yang, A.B. Bocarsly, S. Srinivasan, *Electrochim. Acta*, 47, 1023 (2002).
- [8] Q. Li, R. He, J.O. Jensen, and N.J. Bjerrum, *Chem. Mater.*, 15, 4896 (2003).
- [9] S.H. Kwak, T.H. Yang, C.S. Kim, and K.H. Yoon, *Solid State Ionics*, 160, 309 (2003).
- [10] Y. Si, H.R. Kunz, and J.M. Fenton, *J. Electrochem. Soc.*, 151, 623 (2004).
- [11] J.A. Asensio, S. Borrós, and P. Gómez-Romero, *J. Electrochem. Soc.*, 151, 304 (2004).
- [12] O. Nishikawa, T. Sugimoto, S. Nomura, K. Doyama, K. Miyatake, H. Uchida, and M. Watanabe, *Electrochim. Acta*, 50, 667 (2004).
- [13] K. Tadanaga, H. Yoshida, A. Matsuda, T. Minami, and M. Tatsumisago, *Electrochim. Acta*, 50, 705 (2004).
- [14] V. Ramani, H.R. Kunz, and J.M. Fenton, *Electrochim. Acta*, 50, 1181 (2005).
- [15] M.A. Sweikart, A.M. Herring, J.A. Turner, D.L. Williamson, B.D. McCloskey, S.R. Boonrueng, and M. Sanchez, *J. Electrochem. Soc.*, 152, 98 (2005).
- [16] V. Baglio, A.S. Arico, A.D. Blasi, V. Antonucci, P.L. Antoucci, S. Licoccia, E. Traversa, and F.S. Fiory, *Electrochim. Acta*, 50, 1241 (2005).
- [17] K.T. Adjemian, S.J. Lee, S. Srinivasan, J. Benziger, A.B. Bocarsly, *J. Electrochem. Soc.*, 149, 256 (2002).
- [18] H. Nakajima, S. Nomura, T. Sugimoto, S. Nishikawa, and I. Honma, *J. Electrochem. Soc.*, 149, 953 (2002).
- [19] I. Honma, H. Nakajima, O. Nishikawa, T. Sugimoto, and S. Nomura, *J. Electrochem. Soc.*, 149, 1389 (2002).
- [20] K.D. Kreuer, *Chem. Mater.*, 8, 610 (1996).
- [21] A.M. Grillone, S. Panero, B.A. Retamel, and B. Scrosati, *J. Electrochem. Soc.*, 146, 27 (1999).
- [22] J.-Y. Sanchez, A. Denoyelle, and C. Poinsignon, *Polym. Adv. Technol.*, 4, 99 (1993).
- [23] W.A. England, M.G. Cross, A. Hamnett, P.J. Wiseman, and J.B. Goodenough, *Solid State Ionics*, 1, 231 (1980).
- [24] K.D. Kreuer, M. Hampele, K. Dolde, and A. Rabenau, *Solid State Ionics*, 28/30, 589 (1988).
- [25] M. Tatsumisago, H. Honjo, Y. Sakai, and T. Minami, *Solid State Ionics*, 74, 105 (1994).
- [26] I. Honma, S. Hirakawa, K. Yamada, and J.M. Bae, *Solid State Ionics*, 118, 29 (1998).
- [27] I. Honma, Y. Takeda, and J.M. Bae, *Solid State Ionics*, 120, 255 (1999).
- [28] I. Honma, S. Nomura, and H. Nakajima, *J. Membr. Sci.*, 185, 83 (2001).
- [29] M. Doyle, S.K. Choi, and G. Proulx, *J. Electrochem. Soc.*, 147, 34 (2000).
- [30] J.-T. Wang, R.F. Savinell, J. Wainright, M. Litt, and H. Yu, *Electrochim. Acta*, 41, 193 (1996).
- [31] K.D. Kreuer, A. Fuchs, M. Ise, M. Spaeth, and J. Maier, *Electrochim. Acta*, 43, 1281 (1998).
- [32] J.J. Fontanella, M.C. Wintersgill, J.S. Wainright, R.F. Savinell, and M. Litt, *Electrochim. Acta*, 43, 1289 (1998).

- [33] T. Kobayashi, M. Rikukawa, K. Sanui, and N. Ogata, *Solid State Ionics*, 106, 219 (1998).
- [34] P.L. Antonucci, A.S. Arico, P. Creti, E. Ramunni, and V. Antonucci, *Solid State Ionics*, 125, 431 (1999).
- [35] X. Ren, M.S. Wilson, and S. Gottesfeld, *J. Electrochem. Soc.*, 143, L12 (1996).
- [36] P. Staiti, M. Minutoli, and S. Hocevar, *J. Power Sources*, 90, 231 (2000).
- [37] G. Alberti, M. Casciola, L. Massinelli, and B. bauer, *J. Membr. Sci.*, 185, 73 (2001).
- [38] K.D. Kreuer, *J. Membr. Sci.*, 185, 29 (2001).
- [39] D.J. Jones and J. Roziere, *J. Membr. Sci.*, 185, 41 (2001).
- [40] S. Haufe and U. Stimming, *J. Membr. Sci.*, 185, 95 (2001).
- [41] J.D. Kim, and I. Honma, *J. Electrochem. Soc.*, 151, 1396 (2004).
- [42] D.A. Loy, G.M. Jamison, B.M. Baugher, S.A. Myers, R.A. Assink, and K.J. Shea, *Chem. Mater.*, 8, 656 (1996).
- [43] H.-H. Huang, B. Orlor, and G.L. Wilkes, *Macromolecules*, 20, 1322 (1987).
- [44] H. Schmidt, *J. Non-Crystalline Solids*, 73, 681 (1985).
- [45] J.D. Mackenzie, Y.J. Chung, and Y. Hu, *J. Non-Crystalline Solids*, 147/148, 271 (1992).
- [46] S. Katayama, Y. Kubo, and N. Yamada, *J. Am. Ceram. Soc.*, 85, 1157 (2002).
- [47] K.J. Shea, and D.A. Loy, *MRS Bull.*, 26, 368 (2001).
- [48] I. Honma, H. Nakajima, O. Nishikawa, T. Sugimoto, and S. Nomura, *J. Electrochem. Soc.*, 150, 616 (2003).
- [49] Y.-I. Park, and M. Nagai, *Solid State Ionics*, 145, 149 (2001).
- [50] J.D. Kim, and I. Honma, *Electrochim. Acta*, 48, 3633 (2003).
- [51] J.D. Kim, and I. Honma, *Electrochim. Acta*, 49, 3429 (2004).
- [52] J.D. Kim, and I. Honma, *Electrochim. Acta*, 49, 3179 (2004).
- [53] J.D. Kim, and I. Honma, *Solid State Ionics*, 176, 547 (2005).
- [54] J.D. Kim, and I. Honma, *Solid State Ionics*, 176, 979 (2005).
- [55] J.D. Kim, T. Mori, and I. Honma, *J. Electrochem. Soc.*, 153, 508 (2006).
- [56] E. Coronado, and C.J. G-Garcia, *Chem. Rev.*, 98, 273 (1998).
- [57] O. Nakamura, T. Kodama, I. Ogino, and Y. Miyake, *Chem. Lett.*, 17 (1979).
- [58] K. Segawa, S. Nakata, and S. Asaoka, *Mater. Chem. Phys.* 17, 195 (1987).
- [59] M.M. Mastikhin, and S.M. Timofeeva, *J. Mol. Catal.* 60, 65 (1990).

(Received December 9, 2007 ; Accepted September 1, 2008)